Strain enhancement of the electro-optical response in BaTiO_{3} films integrated on Si(001)

Kurt D. Fredrickson, Viola Valentina Vogler-Neuling, Kristy J. Kormondy, Daniele Caimi, Felix Eltes, Marilyne Sousa, Jean Fompeyrine, Stefan Abel, and Alexander A. Demkov

Phys. Rev. B **98**, 075136 — Published 20 August 2018

DOI: 10.1103/PhysRevB.98.075136

Strain enhancement of the electro-optical response in $BaTiO_3$ films integrated on Si (001)

Kurt D. Fredrickson[1*], Viola Valentina Vogler-Neuling[2†], Kristy J. Kormondy[1‡], Daniele Caimi[2], Felix Eltes[2], Marilyne Sousa[2], Jean Fompeyrine[2], Stefan Abel[2], and Alexander A. Demkov[1§]

[1]Department of Physics, The University of Texas at Austin, Austin, TX 78712, USA

[2]IBM Research-Zurich, Säumerstrasse 4, 8803 Rüschlikon, Switzerland

Abstract

We discuss the possibility of significantly enhancing the nonlinear electro-optical response in strained perovskite $BaTiO_3$. First principles calculations predict the enhancement for both compressive and tensile strain. The physical origin can be traced to strain-induced phonon softening that results in diverging first order susceptibility. Within the Landau-Ginzburg-Devonshire formalism we demonstrate how, in turn, this divergence results in a diverging second order susceptibility and Pockels coefficient. Our results suggest a way to optimize $BaTiO_3$ films for use in silicon nanophotonics.

I. Introduction

Interest in $BaTiO_3$ (BTO) for use in nonlinear optic devices lies in its extremely large electro-optic (Pockels) coefficients >100 pm/V.[1,2] Even more importantly, the monolithic integration of BTO on semiconductors has paved the way to several types of entirely different devices ranging from ferroelectric memory to electro optical modulators.[3] Together, these developments have raised a possibility for applications of BTO in silicon nanophotonics, a hybrid technology combining semiconductor logic with fast broadband optical communications and optical information technologies.[1,4–6]

BTO is a perovskite that has originally garnered interest for integration on semiconductors, due to its very high permittivity.[7] It has been grown epitaxially on Si(001) using BaO,[8] $Ba_{0.7}Sr_{0.3}TiO_3$ (BST),[9] and $SrTiO_3$ (STO)[10–12] buffer layers, and on Ge both directly[13] or with an STO[14] buffer layer. Above the Curie temperature of ~120ºC, BTO is cubic and paraelectric, but below that temperature, it becomes tetragonal and ferroelectric.[15–17] The ferroelectric transition from cubic

* Current address: Patterson+Sheridan LLC, San Jose, CA 95113, USA

† Current address: Optical Nanomaterial Group, Institute for Quantum Electronics, Department of Physics, ETH Zurich, Auguste-Piccard Hof 1, 8093 Zurich, Switzerland

‡ Current address: Intel, Inc. Hillsboro, OR 97003, USA

§demkov@physics.utexas.edu

(*m3m*) to tetragonal (*4mm*) symmetry is believed to be first order but close to second order and is described by a multicomponent order parameter, which is directly proportional to polarization.[18]

The dielectric constant ε of BTO diverges upon approaching the Curie temperature.[19] Previous theoretical studies have shown that strain can soften the phonon modes, also resulting in diverging ε in $SrTiO_3$[20] as well as in BTO[21]. Particularly, in BTO this divergence occurs near the strain-induced monoclinic-to-orthorhombic phase transition[21]. The Pockels or *linear electro optic-effect* occurs in certain non-centrosymmetric crystals, such as BTO, and describes a change in ε caused by applied electric field:

$$\Delta\left(\frac{1}{\varepsilon}\right)_{ij} = \sum_k r_{ijk} E_k, \qquad (1)$$

where $\boldsymbol{r}$ is the electro-optic tensor. Importantly, the Pockels effect in thin BTO films integrated on Si (001) enables optical on-chip manipulation of information at telecom wavelength of 1.55 μm.[1,4,6] As the thin film is grown epitaxially on a substrate with a lesser lattice constant, the effect of strain on the electro-optical properties is of crucial importance. There has been some theoretical[22–26] and experimental work[27,28] on the electro-optic tensor of BTO, but so far the effect of strain has not received appropriate attention.

Here, using first principles calculations and Landau-Ginzburg-Devonshire theory we demonstrate that in BTO films integrated on a Si (001) substrate, strain causes divergence in first and second order susceptibility, which in turn significantly enhances the electro-optic effect, thus making Si-integrated BTO extremely attractive for applications in Si nanophotonics.

II. Theoretical calculations

Using density functional theory (DFT), we calculate the effect of strain on the dielectric tensor and nonlinear electro-optic tensor of BTO, considered as an epitaxial strained film. All calculations are done using DFT within the local density approximation (LDA) as implemented in the ABINIT code, using Teter norm-conserving extended pesudoptentials;[29] we use density functional perturbation theory to calculate phonon frequencies and eigenvectors, along with the calculation of ε and r.[23,30,31] We use the valence configuration $5s^2 5p^6 6s^2$ for Ba, $3s^2 3p^6 4s^2 3d^2$ for Ti, and $2s^2 2p^4$ for O. We use a 1220 eV kinetic energy cutoff for the plane wave expansion. For the Brillouin zone integration, we use dense 10×10×10 Monkhorst-Pack[32] k-point meshes. As the polarization is sensitive to the lattice constant, and is adversely affected by its underestimation in the LDA,[33] we choose to work with the experimental room temperature tetragonal crystal structure with lattice constants of a = 3.994 Å and c = 4.038 Å.[34] We also use the experimental elastic constants (222 GPa for C_{11}, 108 GPa for C_{12}, 111 GPa for C_{13} and 151 GPa for C_{33}[27]) to account for strain. We model two cases (Figure 1): the first is when the BTO film is polarized out-of-plane, with the long c axis perpendicular to the BTO/Si interface; accordingly, we strain the a and b lattice constants uniformly (so that $a = b$ for all strains), and use elastic constants to find the optimum c lattice constant. In the second case, BTO is in-plane polarized, with the long c axis parallel to the interface; we strain the a and c lattice constants by the same amount, and

use elastic constants to find the optimum b lattice constant (in this case, in general $a \neq b \neq c$, but c/a is fixed). In all cases we relax the ions until the forces are less than 1×10^{-4} eV/Å.

A few words need to be said about the calculations of the electro-optical tensor, as it is not trivial for bulk BTO. Fortunately, the problem we are interested in, i.e. the strain effect on the nonlinear response in an epitaxial film, is somewhat more tractable. Still, the results are only qualitative, despite the first principles nature of the theory. For our purposes, it is sufficient to consider a strain-free (clamped) response. In other words, we ignore the piezoelectric contribution to the EO tensor.[35] Most importantly, the calcualtions are limited to zero Kelvin, and the primitive tetragonal *P4mm* cell is dynamically unstable and therefore, it is not posssible to compute the largest bulk r_{42} component, as has ben poined out by Veithen *et al*.[23] We obtain the bulk values of r_{13} and r_{33} to be 9.2 and 23.6 pm/V, respectively, close to 8.9 and 22.3 pm/V, the clamped LDA result of Veithen *et al*.[23] These should be compared with 10.2 and 40.6 pm/V reported by Zgonik *et al*.[36] The origin of this discrepancy is subtle, and can be traced to the zero Kelvin nature of the calculation. The room temperature five-atom *P4mm* cell of ferroelectric BTO is actually a dynamic time average over the fluctuating lower symmetry structures;[37] and it is this structure that gives a large EO reponse. At low temperature, corresponding to the calculation, the ground state structure of BTO is the low symmetry *R3m* structure. Therefore, the bulk response is computed for an average cell that doesn't represent the instantaneous bulk crystal at room temperature. Fortunately, the strain effect we are after is governed by the soft mode mechanism[20,21], not the order-disorder mechanism of the bulk crystal. Therefore, despite these limitations of the theory, the change in the EO response caused by epitaxial strain is captured reasonably well. Thus, though the absolute values should be taken with a grain of salt, the physics will be properly described and our calculation provides a qualitative description of the EO response of BTO under strain.

III. Discussion

First, we discuss the case when the BTO film is polarized out-of-plane, with the long c axis perpendicular to the BTO/Si interface; accordingly, we strain the a and b lattice constants uniformly (so that $a = b$ for all strains), and use elastic constants to find the optimum c lattice constant (Figure 2(a)). In ferroelectrics, the rumpling is defined as the difference between the O and Ti positions in the direction of interest (to a good approximation, the polarization of the system is linear with respect to the rumpling of the cell).[38] In Figure 2b, we show the effect of strain on the atomic rumpling where BTO is polarized normal to the interface. We note that, even in the unstrained case, BTO is polarized not only in the long axis c direction, but the Ti and O had displacements also along the a and b directions, although to a lesser degree. A previous experimental study showed that BTO polarization does not directly point toward the [111] axis, but is slightly tilted away by $11.7 \pm 1.1°$ toward the xy-plane, as the c direction rumpling is larger than in the a or b direction.[39] In the unstrained case, we calculate an off-angle of 10.7°, in excellent agreement with the previous experimental results. In Figure 2b, we see that there are two critical strain values in the system: One at -1% compressive strain, where the rumpling in the

a and *b* directions vanish, and one at 1.3% tensile strain, where the rumpling in the *c* direction vanishes. At above ~1.3%, the rumpling in the [001] direction vanishes, and only the [110] rumpling remains; below -0.5% strain, the rumpling in the [110] vanishes, and only the [001] rumpling remains; for strains below 1.3% and above -0.5%, there is rumpling in both directions. Interestingly, these transitions do not occur when the *a/c* ratio becomes smaller than 1, which occurs at ~ 0.5% strain. This shows that the disappearance of rumpling in certain directions is not related to the change in long cell axis (switching from *c* being the long axis to the *a* and *b* axes being the long axes).

In Figure 3a, we show the dielectric tensor ε as a function of strain where BTO is polarized perpendicular to the interface ($\varepsilon_{11} = \varepsilon_{22}$ by symmetry). We see that at -1.0% strain, ε_{11} diverges, and at 1.3% strain, ε_{33} diverges. These are the same strains for which the *a/b* rumpling and *c* rumpling vanish. The reason for the divergences is the softening of phonon modes. In Table 1, we show that the [110] ferroelectric mode (in which the Ti moves in the [110] direction, and the O move in the $[\bar{1}\,\bar{1}0]$ direction) softens as we approach the critical strain, either from below -1.0% of strain or above. This can be thought of in terms of the Lyddane-Sachs-Teller or LST relation[40,41], as the frequency of one of the ω_{TO} decreases toward zero, ε diverges (in this case only one element of the ε tensor). Likewise, in Table 2 we show that the [001] ferroelectric mode (in which the Ti moves in the [001] direction, and the O move in the $[00\bar{1}]$ direction) softens as we approach the critical strain of 1.3%. This is similar to the result of Reference[21]. However, while the BTO undergoes a phase transition to a cell of a different symmetry, we keep the BTO in our calculations tetragonal to model clamping on a substrate.

Table 1. The frequency of the ferroelectric mode in the [110] direction with respect to strain, for the out-of-plane polarized case.

Strain	Frequency (1/cm)
-1.20%	62.40
-1.15%	57.47
-1.10%	47.54
-1.05%	36.30
-1.00%	37.34
-0.90%	52.22
0%	157.59

Table 2. The frequency of the ferroelectric mode in the [001] direction with respect to strain, for the out-of-plane polarized case.

Strain	Frequency (1/cm)
0%	282.94
1.10%	109.16
1.20%	68.47

1.30%	21.27
1.50%	81.62
1.60%	100.05

Next, we calculate the ***r*** tensor as a function of strain. In Figure 3b, we report the values of $r_{113,}$ $r_{333,}$ and $r_{232} = r_{131,}$ ($r_{13} = r_{23}$, r_{33}, and $r_{42} = r_{51}$ respectively, in Voigt notation). The *r* tensor can be separated into two components: the electronic part r^{el}, and the ionic part r^{ion}. The r^{ion} is given by

$$r_{ijk}^{ion} = \frac{-4\pi}{\sqrt{V} n_{ii}^2 n_{jj}^2} \sum_m \frac{\alpha_{ij}^m p_k^m}{\omega_m^2}, \quad (2)$$

where V is the unit cell volume, n is the index of refraction, α_m is the Raman susceptibility of mode m given by

$$\alpha_{ij}^m = \sqrt{V} \sum_{\kappa,\beta} \frac{\partial \chi_{ij}^{(1)}}{\partial \tau_{\kappa,\beta}} u_m(\kappa,\beta), \quad (3)$$

where κ indexes the atoms in a unit cell, β is a Cartesian direction, $\chi^{(1)}$ is the linear susceptibility tensor, $\tau_{\kappa\beta}$ is the displacement of atom κ in the β direction, and u is the displacement pattern of the eigenmode m. p is the mode polarity given by

$$p_i^m = \sum_{\kappa,j} Z_{\kappa,ij}^* u_m(\kappa, j) \quad (4)$$

where Z^* is the Born effective charge tensor.[23] The electronic part r^{el} is small (less than 3 pm/V for all values of strain considered) and is not important for the following discussion. Previous theoretical calculations of *r* for BTO found a value of 8.9 pm/V for r_{13} and a value of 22.3 pm/V for r_{33} for unstrained BTO.[22] In comparison, we calculate a value of 0.5 pm/V for r_{13}, and a value of 24.0 pm/V for r_{33}. Although the values of r_{33} are in good agreement, our value of r_{13} is smaller than the previous result. This is because the previous calculation did not take into account the rumpling in the *a* and *b* directions (the imaginary frequencies of these modes were not included in the calculation of the *r* tensor in Equation 2 above). Our calculations show that these modes have a large contribution to *r* that actually cancels the contributions from other modes in the system, resulting in a reduced value of r_{13}.

Although r_{13} varies with strain, it always stays smaller than 8 pm/V. In contrast, r_{33} and r_{42} diverge at 1.3% and -1.0% strain, respectively. This is precisely where the divergence of ε_{33} and ε_{11} occurs. From Equation 2, we see that r^{ion} depends strongly on the frequency of the modes of the system, and a softening mode increases the electro-optic response of the crystal. We calculate the contribution of specific phonons to the *r* tensor, and find that the modes that have a large contribution to *r* are the same modes as listed in Table 1. This shows that the modes that soften due to strain and cause divergence in ε are the same modes that cause divergence of *r*.

Let us now consider the case of BTO polarized parallel to the interface (in transmission, the electric field of light is parallel to the film surface and would not couple to polarization normal to the surface/interface). The long *c* axis lies in-plane along with the *a* lattice vector, while the *b* lattice vector is perpendicular to the interface; alternating mutually orthogonal domains of *c*-oriented BTO have been described as a mosaic structure.[42] In this case, we strain *a* and *c* so that the *a/c* ratio is fixed, and use the elastic constants to optimize the *b* lattice vector, Figure 4(a). Under this strain, the crystal becomes orthorhombic, and so $\varepsilon_{11} \neq \varepsilon_{22} \neq \varepsilon_{33}$. In Figure 4(b), we plot the rumpling in this cell under various *a*/*c* strains. There are again two critical strains in the system; one at -1.0% strain, where the polarization in the *a* direction vanishes, and one at 0.8% strain, where the polarization in the *b* direction vanishes. In Figure 5(a), we plot the dielectric constant as a function of strain. Now, we see that ε_{11} diverges at -1.0%, where the *a* polarization vanishes, and ε_{22} diverges at 0.8%, where the *b* polarization vanishes, consistent with our results for the out-of-plane polarization. In Table 3, we show that the [100] ferroelectric mode (in which the Ti moves in the [100] direction, and the O move in the $[\bar{1}00]$ direction) softens as we approach the critical strain, either from below -1.0% of strain or from above. Likewise, in Table 4 we show that the [010] ferroelectric mode (in which the Ti moves in the [010] direction, and the O move in the $[0\bar{1}0]$ direction) softens as we approach the critical strain of 0.8%.

In Figure 5b, we plot the components of the electro-optic tensor as a function of strain. Unlike in the previous example, under orthorhombic strain, r_{51} and r_{42} are no longer equal. We see that r_{51} diverges at -1.0% strain, and r_{42} diverges at 0.8% strain, again corresponding to the polarization vanishing in one of the crystal directions and of the divergence of ε. Again, the modes that have a large contribution to *r* are the modes soften due to strain.

Table 3. The frequency of the ferroelectric mode in the [100] direction with respect to strain, for the in-plane polarized case.

Strain	Frequency (1/cm)
-1.20%	64.30
-1.10%	52.87
-1.00%	36.29
-0.90%	47.75
-0.80%	76.56

Table 4. The frequency of the ferroelectric mode in the [010] direction with respect to strain, for the in-plane polarized case.

Strain	Frequency (1/cm)
0.60%	93.75
0.70%	66.75
0.80%	32.83

0.90%	48.77
1.00%	64.78

This relationship between the large Pockels effect and mode softening can be understood within the Landau-Ginzburg-Devonshire theory.[20,43–48] In this theory, the free energy density F is given by:

$$F(P,T) = F_0 + \frac{1}{2}\alpha P^2 + \frac{1}{4}\beta P^4 , \quad (5)$$

where F_0 is the free energy density at zero polarization, P is the polarization, and α and β are coefficients that depend on temperature and strain. The electric field E is given by

$$E = \frac{\partial F}{\partial P} = \alpha P + \beta P^3 . \quad (6)$$

The linear susceptibility $\chi^{(1)}$ is defined as

$$\chi^{(1)} = \frac{\partial P}{\partial E} = \left(\frac{\partial E}{\partial P}\right)^{-1} = \frac{1}{\alpha + 3\beta P^2} , \quad (7)$$

and

$$\varepsilon = 1 + \chi^{(1)} , \quad (8)$$

where the dielectric function ε measures the linear response. As BTO also has a nonlinear dielectric response to an electric field, one can readily compute the nonlinear electric susceptibly $\chi^{(2)}$ as[49] (the tensor notations are omitted for clarity):

$$\chi^{(2)} = \frac{\partial^2 P}{\partial E^2} = -\frac{\partial^2 E}{\partial P^2}\left(\frac{\partial P}{\partial E}\right)^3 = -6\beta P\left(\chi^{(1)}\right)^3 \quad (9)$$

This means that ε changes with respect to an additional applied field E, giving us a change in the dielectric tensor $\Delta\varepsilon$ that depends on the strength of E. This is the Pockels effect and the electro-optic tensor r is related to $\Delta\varepsilon$ as:

$$rE = \Delta\left(\frac{1}{\varepsilon}\right) \approx \frac{-\Delta\varepsilon}{\varepsilon^2} = \frac{-\chi^{(2)}E}{(1+\chi^{(1)})^2} = \frac{3\beta P(\chi^{(1)})^3 E}{(1+\chi^{(1)})^2} \quad (11)$$

It is clear that the divergence of r must occur if $\chi^{(1)}$ and ε diverge. In our case, the physical reason for the susceptibility divergence is the strain-induced-softening of the corresponding phonon mode.

We also performed preliminary experimental investigation of Pockels coefficients dependence on strain in a BTO film integrated on Si (001) that will be published separately. The tentative results are in qualitative agreement with theoretical predictions. Just a -0.04% change in relative strain causes a 30 pm/V increase in the effective Pockels coefficient. The calculated response to strain can be inferred from Fig. 5b, we obtain a change of 117 pm/V in the r_{51} value when the strain increases from -0.8% to -0.9%. It is instructive to compare the effect of strain with that of

temperature. Bernasconi and co-authors have related the temperature dependence of the linear EO coefficient to changes in the dielectric tensor and spontaneous polarization.[26] They argue that in BTO and $KNbO_3$ the temperature dependence is dominated by the variation in the permittivity, which is amplified by a structural instability. This is similar to what happens under strain according to our calculations. Also, when the lattice instability is caused by epitaxial strain there is no ambiguity to whether the transition is order-disorder or soft-mode type, as there is a specific divergent mode responsible for it.

Conclusion

In conclusion, we show that in strained epitaxial BTO films, for both normal and in plane polarization, the Pockels effect is enhanced under strain due to divergence of dielectric susceptibility. The divergence is caused by strain-induced soft modes and is manifested by an extinguishing of polarization in certain directions under strain. Based on the relation between the linear and nonlinear susceptibilities in the Landau-Ginzburg-Devonshire theory, we expect this divergence of *nonlinear response* caused by mode softening to be quite general. The first principles calculations suggest very large electro-optic effects that can be obtained via control of the lattice mismatch to the substrate. Our results suggest a previously unexplored route of tuning the electro-optic effect in active elements of Si nanophotonics.

We thank Agham Posadas and Ali Hamze for critically reading the manuscript and insightful discussions. This work was supported by the National Science Foundation (Awards DMR-1207342 and IRES-1358111), the Air Force Office of Scientific Research (Grant FA9550–12–10494), Texas Advanced Computing Center, and the European Commission (FP7-ICT-2013-11-619456-SITOGA, H2020-ICT-2015-25-688579 PHRESCO).

References

[1] S. Abel, T. Stöferle, C. Marchiori, C. Rossel, M. Rossell, R. Erni, D. Caimi, M. Sousa, A. Chelnokov, B. Offrein, and J. Fompeyrine, Nat. Commun. **4**, 1671 (2013).

[2] P. Tang, D.J. Towner, T. Hamano, A.L. Meier, and B.W. Wessels, Opt. Express **12**, 5962 (2004).

[3] A.A. Demkov and A.B. Posadas, *Integration of Functional Oxides with Semiconductors* (Springer New York, New York, NY, 2014).

[4] C. Xiong, W.H.P. Pernice, J.H. Ngai, J.W. Reiner, D. Kumarh, F.J. Walker, C.H. Ahn, and H.X. Tang, Nano Lett. **14**, 1419 (2014).

[5] K.J. Kormondy, S. Abel, F. Fallegger, Y. Popoff, P. Ponath, A.B. Posadas, M. Sousa, D. Caimi, H. Siegwart, E. Uccelli, L. Czornomaz, C. Marchiori, J. Fompeyrine, and A.A. Demkov, Microelectron. Eng. **147**, 215 (2015).

[6] K.J. Kormondy, Y. Popoff, M. Sousa, F. Eltes, D. Caimi, M.D. Rossell, M. Fiebig, P. Hoffmann, C. Marchiori, M. Reinke, M. Trassin, A.A. Demkov, J. Fompeyrine, and S. Abel, Nanotechnology **28**, 075706 (2017).

[7] J. Robertson, Reports Prog. Phys. **69**, 327 (2006).

[8] R.A. McKee, F.J. Walker, and M.F. Chisholm, Science **293**, 468 (2001).

[9] V. Vaithyanathan, J. Lettieri, W. Tian, A. Sharan, A. Vasudevarao, Y.L. Li, A. Kochhar, H. Ma, J. Levy, P. Zschack, J.C. Woicik, L.Q. Chen, V. Gopalan, and D.G. Schlom, J. Appl. Phys. **100**, 024108 (2006).

[10] F. Niu and B.W. Wessels, J. Vac. Sci. Technol. B **25**, 1053 (2007).

[11] C. Dubourdieu, J. Bruley, T.M. Arruda, A. Posadas, J. Jordan-Sweet, M.M. Frank, E. Cartier, D.J. Frank, S. V Kalinin, A.A. Demkov, and V. Narayanan, Nat. Nanotechnol. **8**, 748 (2013).

[12] S. Abel, T. Stöferle, C. Marchiori, C. Rossel, M.D. Rossell, R. Erni, D. Caimi, M. Sousa, A. Chelnokov, B.J. Offrein, and J. Fompeyrine, Nat. Commun. **4**, 1671 (2013).

[13] K.D. Fredrickson, P. Ponath, A.B. Posadas, M.R. McCartney, T. Aoki, D.J. Smith, and A.A. Demkov, Appl. Phys. Lett. **104**, 242908 (2014).

[14] P. Ponath, K. Fredrickson, A.B. Posadas, Y. Ren, X. Wu, R.K. Vasudevan, M. Baris Okatan, S. Jesse, T. Aoki, M.R. McCartney, D.J. Smith, S. V. Kalinin, K. Lai, and A.A. Demkov, Nat. Commun. **6**, 6067 (2015).

[15] B. Wul and I.M. Goldmand, C. R. Acad. Sci. URSS **46**, 139 (1945).

[16] B. Wul and I.M. Goldmand, C. R. Acad. Sci. URSS **49**, 177 (1945).

[17] B. Wul and I.M. Goldmand, C. R. Acad. Sci. URSS **51**, (1946).

[18] B.A. Strukov and A.P. Levanyuk, *Ferroelectric Phenomena in Crystals* (Springer Berlin Heidelberg, Berlin, Heidelberg, 1998).

[19] W.J. Merz, Phys. Rev. **76**, 1221 (1949).

[20] A. Antons, J.B. Neaton, K.M. Rabe, and D. Vanderbilt, Phys. Rev. B **71**, 024102 (2005).

[21] P. V. Ong and J. Lee, J. Appl. Phys. **112**, 014109 (2012).

[22] M. Veithen, X. Gonze, and P. Ghosez, Phys. Rev. Lett. **93**, 187401 (2004).

[23] M. Veithen, X. Gonze, and P. Ghosez, Phys. Rev. B **71**, 125107 (2005).

[24] S. Cabuk, Cent. Eur. J. Phys. **10**, 239 (2012).

[25] A. Mamedov and E. Ozbay, ArXiv:1112.5851 (n.d.).

[26] P. Bernasconi, M. Zgonik, and P. Gunter, J. Appl. Phys. **78**, 2651 (1995).

[27] M. Zgonik, P. Bernasconi, M. Duelli, R. Schlesser, P. Günter, M.H. Garrett, D. Rytz, Y. Zhu, and X. Wu, Phys. Rev. B **50**, 5941 (1994).

[28] S.H. Wemple and D. DiDomenico, *Applied Solid State Science* (Academic, New York, 1972).

[29] M. Teter, Phys. Rev. B **48**, 5031 (1993).

[30] X. Gonze, B. Amadon, P.M. Anglade, J.M. Beuken, F. Bottin, P. Boulanger, F. Bruneval, D. Caliste, R. Caracas, M. Côté, T. Deutsch, L. Genovese, P. Ghosez, M. Giantomassi, S. Goedecker, D.R. Hamann, P. Hermet, F. Jollet, G. Jomard, S. Leroux, M. Mancini, S. Mazevet, M.J.T. Oliveira, G. Onida, Y. Pouillon, T. Rangel, G.M. Rignanese, D. Sangalli, R. Shaltaf, M. Torrent, M.J. Verstraete, G. Zerah, and J.W. Zwanziger, Comput. Phys. Commun. **180**, 2582 (2009).

[31] D.R. Hamann, X. Wu, K.M. Rabe, and D. Vanderbilt, Phys. Rev. B **71**, 035117 (2005).

[32] H.J. Monkhorst and J.D. Pack, Phys. Rev. B 5188 (1976).

[33] R.E. Cohen, Nature **358**, 136 (1992).

[34] I.K. Jeong, S. Lee, S.Y. Jeong, C.J. Won, N. Hur, and A. Llobet, Phys. Rev. B **84**, 064125 (2011).

[35] J.F. Nye, *Physical Properties of Crystals* (Clarendon Press, Oxford, 2006).

[36] M. Zgonik, P. Bernasconi, M. Duelli, R. Schlesser, P. Günter, M.H. Garrett, D. Rytz, Y. Zhu, and X. Wu, Phys. Rev. B **50**, 5941 (1994).

[37] Y.T. Shao and J.M. Zuo, Acta Crystallogr. Sect. B Struct. Sci. Cryst. Eng. Mater. **73**, 708 (2017).

[38] R. Resta, M. Posternak, and A. Baldereschi, Phys. Rev. Lett. **70**, 1010 (1993).

[39] B. Ravel, E.A. Stern, R.I. Vedrinskii, and V. Kraizman, Ferroelectrics **206–207**, 407 (1998).

[40] R. Lyddane, R. Sachs, and E. Teller, Phys. Rev. **59**, 673 (1941).

[41] W. Cochran, Adv. Phys. **9**, 387 (1960).

[42] Y.L. Li, S.Y. Hu, Z.K. Liu, and L.Q. Chen, Appl. Phys. Lett. **78**, 3878 (2001).

[43] L. Landau, Zh. Eskp. Teor. Fiz. **7**, 627 (1937).

[44] L. Landau, Phys. Z. Sowjun. **11**, 545 (1937).

[45] V. Ginzburg, J. Phys. USSR **10**, 107 (1946).

[46] V. Ginzburg, Zh. Eskp. Teor. Fiz. **19**, 36 (1949).

[47] V. Fridkin and S. Ducharme, *Ferroelectricity at the Nanoscale* (Springer-Verlag Berlin Heidelberg, New York, 2014).

[48] P. Chandra and P.B. Littlewood, ArXiv:Cond-Mat/0609347.

[49] S. Ikeda, H. Kominami, K. Koyama, and Y. Wada, J. App **62**, 3339 (1987).

Figure Captions

Figure 1. (Color online) The unit cell of BTO. In the unstrained case, $a = b < c$. The rumpling and tetragonality of the cell is exaggerated for clarity. We consider two cases; the c-axis pointing perpendicular to the interface (out-of-plane polarization) and the c-axis parallel to the interface (in-plane polarization); in both cases, up on the page corresponds to the direction of the surface. The blue solid line indicates that these axes are strained: The red dashed line indicates the axis that responds to the strain.

Figure 2. (Color online) The lattice parameters (a) rumpling of BTO (b) as a function of strain for the out-of-plane polarized case as shown in schematic above. There are two rumplings for the *a* and *b* directions, since the rumpling for the equatorial O is inequivalent from the rumpling for the apical O. No such complication occurs in the *c*-direction.

Figure 3. (Color online) a) The static dielectric constant and b) electro-optic tensor as a function of strain for the out-of-plane polarized case. Note that at zero strain the r_{42} component of the electro-optic tensor cannot be calculated using the present theory.[22]

Figure 4. (Color online) The lattice parameters (a) and rumpling (b) of BTO as a function of strain for the in-plane polarized case as shown in schematic above. There are two rumplings for all directions, since all three oxygen atoms are inequivalent in an orthorhombic cell. Vertical dashed line indicates experimental lattice parameters.

Figure 5. (Color online) a) The static dielectric constant and b) electro-optic tensor as a function of strain for the in-plane polarized case. Vertical dashed line indicates experimental lattice parameters.

Figures

Figure 1

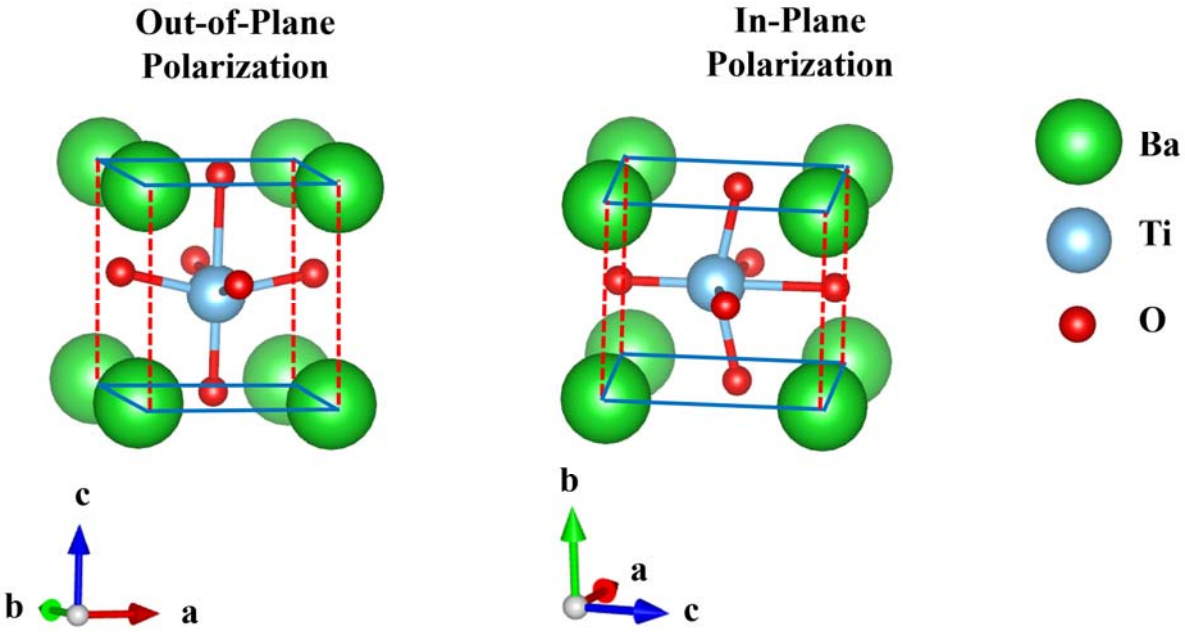

Figure 2

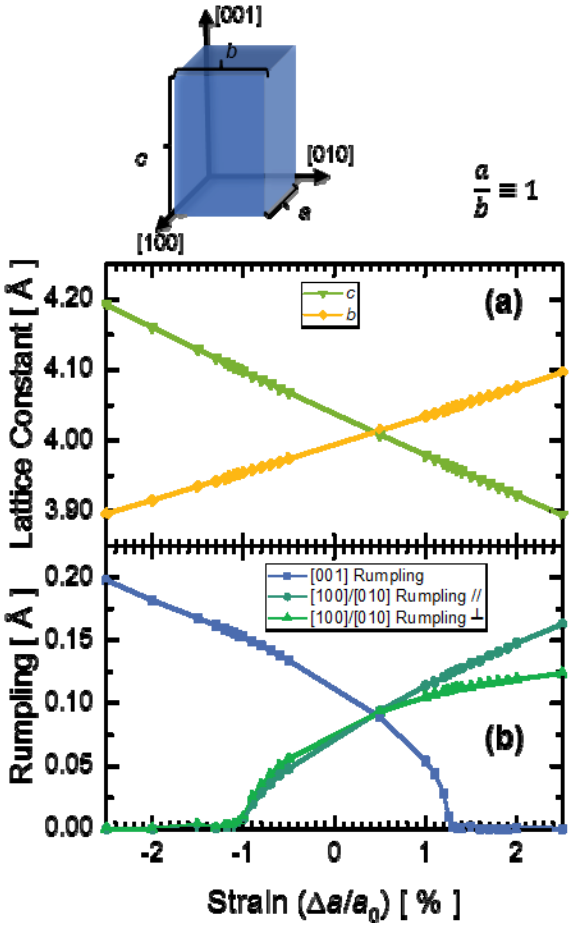
[001]
b
c
[010]
a
[100]
a/b ≡ 1
Lattice Constant [Å]
4.20
4.10
4.00
3.90
c
b
(a)
Rumpling [Å]
0.20
0.15
0.10
0.05
0.00
[001] Rumpling
[100]/[010] Rumpling //
[100]/[010] Rumpling ⊥
(b)
-2
-1
0
1
2
Strain (Δa/a0) [%]

Figure 3

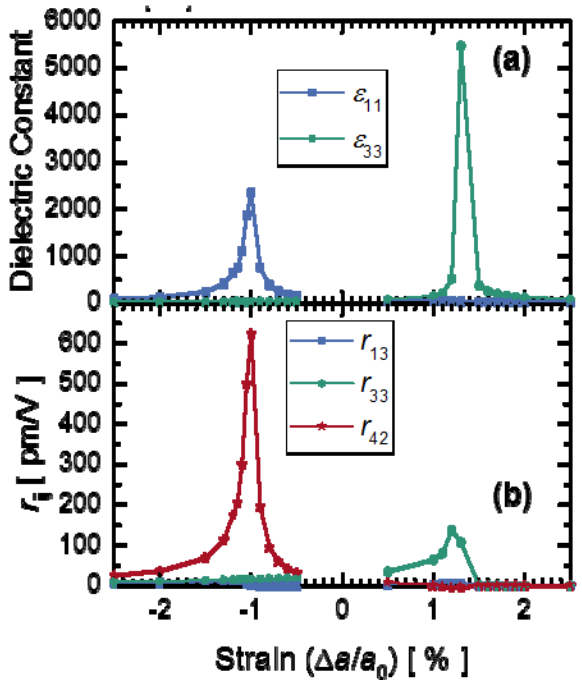
Dielectric Constant
6000
5000
4000
3000
2000
1000
0
(a)
ε_{11}
ε_{33}
r_{ij} [pm/V]
600
500
400
300
200
100
0
r_{13}
r_{33}
r_{42}
(b)
-2
-1
0
1
2
Strain ($\Delta a/a_0$) [%]

Figure 4

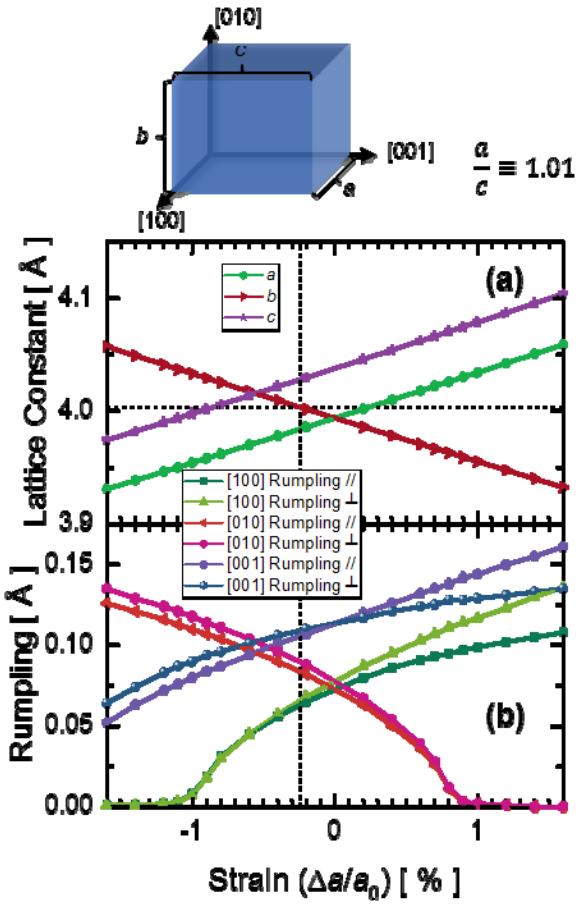
[010]
c
b
[001]
a
[100]
a/c ≡ 1.01
(a)
a
b
c
Lattice Constant [Å]
4.1
4.0
3.9
[100] Rumpling //
[100] Rumpling ⊥
[010] Rumpling //
[010] Rumpling ⊥
[001] Rumpling //
[001] Rumpling ⊥
Rumpling [Å]
0.15
0.10
0.05
0.00
(b)
-1
0
1
Strain (Δa/a0) [%]

Figure 5

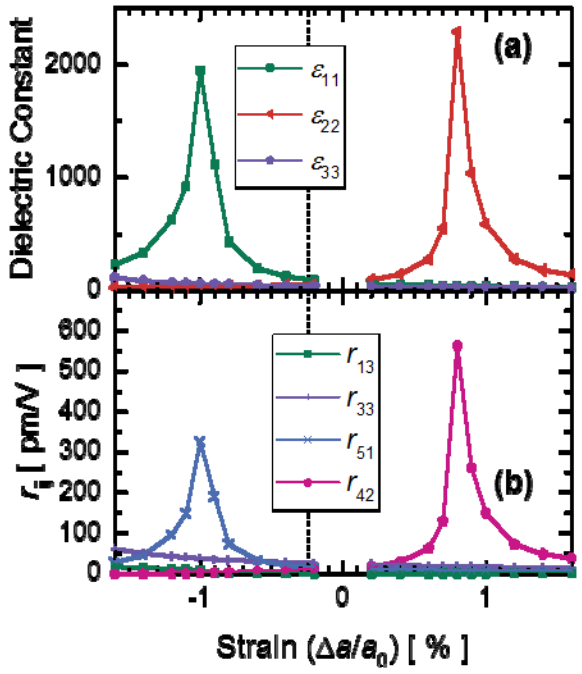
Dielectric Constant
2000
1000
0
ε_{11}
ε_{22}
ε_{33}
(a)
600
500
400
300
200
100
0
r_{ij} [pm/V]
r_{13}
r_{33}
r_{51}
r_{42}
(b)
-1
0
1
Strain ($\Delta a/a_0$) [%]